Pyrene Micropartitioning and Solubilization by Sodium Dodecyl Sulfate Complexes with Poly(ethylene glycol)

Joon-Hyung Kim,[†,‡,§] Michael M. Domach,[‡] and Robert D. Tilton*[,‡,§]

Department of Chemical Engineering and Colloids, Polymers and Surfaces Program, Carnegie Mellon University, Pittsburgh, Pennsylvania 15213

Received: May 25, 1999; In Final Form: October 1, 1999

We examine the effect of poly(ethylene glycol) (PEG) on pyrene solubilization behaviors in aqueous sodium dodecyl sulfate (SDS) solutions. These solutions display strong polymer−surfactant complexation. Following the definitions of Ikeda and Maruyama (*J. Colloid Interface Sci.* **1994**, *166*, 1) we distinguish between the macroscopic solubilizing power and the microscopic solubilization capacity. With pyrene as a model solubilizate, we use ultraviolet absorbance spectrophotometry to measure solubilizing powers. We use excimer fluorescence spectroscopy to identify polymer−surfactant binding transitions and to measure the aggregation numbers of free SDS micelles and of PEG-bound SDS aggregates that contain solubilized pyrene in order to calculate solubilization capacities. The solubilization capacity and solubilizing power of free SDS micelles both increase with increasing aggregation number, when the aggregation number is increased by increasing ionic strength. The solubilization capacity is approximately 3 times more sensitive than the solubilizing power to a change in aggregation number. For a given value of the ionic strength, the aggregation number of a PEG-bound SDS aggregate is approximately 50−60% smaller than that of a free micelle, while its solubilization capacity is within approximately 20% of that of a free micelle. As a result, PEG increases the macroscopic solubilizing power at all SDS concentrations above the critical aggregation concentration by virtue of the greater number of distinct surfactant aggregates formed for a given SDS concentration in the presence of PEG. Compared to free micelles, the solubilizing power of PEG-bound SDS aggregates is significantly more sensitive to ionic strength.

Introduction

Aqueous polymer−surfactant mixtures are of great interest from both fundamental and technological viewpoints. They are encountered in many industrial applications, including water-borne coatings, metal-working fluids, pharmaceutical and personal care product formulations, enhanced oil recovery, and detergency applications. Accordingly, there is considerable practical motivation to understand the effects of polymer−surfactant interactions on the various interfacial phenomena underlying such technologies.

Surfactant binding to polymers in solution has been studied extensively, and much of this work has been reviewed.[1−5] One of the more thoroughly studied model systems for ionic surfactant interactions with nonionic polymers is sodium dodecyl sulfate (SDS) and poly(ethylene glycol) (PEG) or poly(ethylene oxide) (PEO).[6−27] The overall picture for interaction in such a system is that when the surfactant concentration exceeds a critical aggregation concentration (cac), surfactant begins to bind to polymer. The cac is generally lower than the ordinary critical micelle concentration (cmc) that would apply to a pure surfactant solution under otherwise identical conditions. Increasing surfactant concentration leads to increasing polymer−surfactant binding, until the polymer becomes saturated. This occurs at a surfactant concentration c_{sat}. Free micelles do not appear until the total surfactant concentration reaches c_{sat} + cmc − cac, in other words, when the unbound surfactant concentration reaches the cmc.

Solubilization is obviously one of the main applications of surfactants. When surfactants bind to polymers in solution, one naturally expects there to be some effect on solubilization. To describe solubilization phenomena in general, Ikeda and Maruyama[28] defined the (macroscopic) solubilizing power as the number of molecules solubilized per molecule of micellized surfactant. The (microscopic) solubilization capacity is defined as the average number of molecules solubilized in a single micelle at saturation.

Total amounts of solubilization in several different polymer−surfactant systems have been measured over the past few decades.[29−37] Polymer effects have been examined at the macroscopic, or solubilizing power, level, but not at the level of solubilizate micropartitioning between the water pseudophase and the one or more coexisting surfactant pseudophases. Micropartitioning information is essential to evaluate solubilization capacity in polymer−surfactant complexes. For surfactant concentrations between cac and c_{sat}, all solubilization occurs in polymer-bound surfactant aggregates, while at concentrations greater than c_{sat} + cmc − cac, both polymer-bound aggregates and free micelles participate in solubilization. The primary contribution of this paper is to distinguish between solubilizate micropartitioning into free micelles versus polymer-bound surfactant aggregates, to interpret macroscopic solubilizing power measurements in mixtures.

Fluorescence spectroscopy is our primary method to examine SDS−PEG binding and the solubilization capacity for pyrene,

* To whom correspondence should be addressed.
† Current address: Department of Chemical Engineering, Stanford University, Stanford, CA 94305.
‡ Department of Chemical Engineering.
§ Colloids, Polymers and Surfaces Program.

10.1021/jp991720z CCC: $18.00
Published on Web 11/13/1999

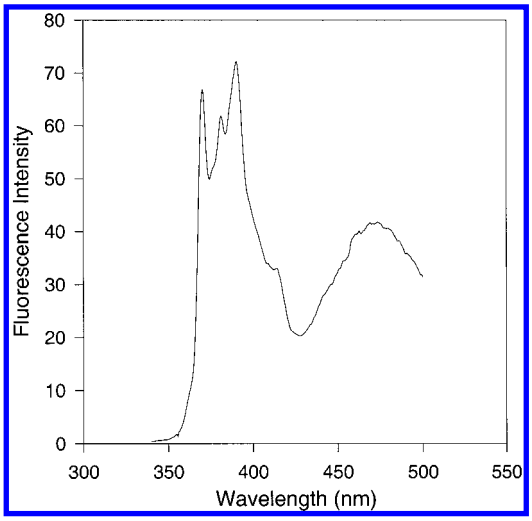

Figure 1. Pyrene fluorescence emission spectrum representative of a micellar SDS solution. Excitation wavelength is 240 nm. Fluorescence intensity has arbitrary units.

a polycyclic aromatic hydrocarbon. We found that the solubilization capacity of free SDS micelles increased proportionately with the micelle aggregation number when ionic strength was increased. For all ionic strengths examined, the solubilization capacities of PEG-bound SDS aggregates were almost the same as those of free SDS micelles, although PEG-bound SDS aggregates have much smaller aggregation numbers. We used UV−vis spectrophotometry to measure the macroscopic solubilizing power. SDS−PEG binding had several effects on solubilization. The first was a trivial result of the fact that the cac is less than the cmc; in SDS−PEG mixtures, the onset of solubilization occurred at total surfactant concentrations that were significantly less than were required in pure SDS solutions. Beyond that, we find that SDS−PEG binding led to enhanced solubilizing power, even though the aggregation number of PEG-bound SDS aggregates was significantly less than that of their unbound counterparts. We also found that the solubilizing power of PEG-bound SDS aggregates was more sensitive than that of free micelles to increasing ionic strength. The overall effect was that more pyrene could be solubilized with less surfactant in the presence of PEG.

Theory

Pyrene, our model solubilizate, has well-known environment-sensitive photophysical characteristics. The pyrene fluorescence emission spectrum has several peaks. Three prominent monomer emission peaks occur at 370 nm (denoted by I_1 or I^{mon}), 380−381 nm (I_3), and 390−391 nm (I_5). When the local concentration of pyrene is high, an excited pyrene molecule can bind a ground-state pyrene molecule and form an excited dimer (excimer). The broad excimer fluorescence emission peak is observed at 470 nm (I^e). A sample emission spectrum that is representative of pyrene solubilized in SDS micelles is shown in Figure 1.

The ratio of two monomer peaks I_1/I_3 is sensitive to the microenvironmental polarity,[38] and the excimer to monomer fluorescence intensity ratio, I^e/I^{mon}, for solubilized pyrene is closely related to its distribution among micelles. Since excimer fluorescence requires dimerization during an excited-state lifetime, a minimum of two pyrenes per micelle is required for solubilized pyrene to produce excimer emission.[39]

The solubilizate distribution among micelles is frequently described by the Poisson distribution model.[40−45] This model assumes that solubilizates are randomly distributed among the micelles. Hunter[46] has analyzed solubilization statistics when instead of a random distribution, there is a finite limit on the number of solubilizates that can be contained within a micelle. In that case, he showed that the binomial distribution is more appropriate. Nevertheless, we and others have shown that the Poisson distribution is an excellent approximation when the average number of solubilizates per micelle is small (less than approximately 5), a condition which is satisfied in the current work.[40,41,44,45,47] Here we use the Poisson distribution, wherein the fraction of micelles containing j solubilized molecules is

$$\frac{[M_j]}{[M]} = \frac{\bar{n}^j e^{-\bar{n}}}{j!} \tag{1}$$

where [M], [M_j], and $\bar{n}$ are the total micelle concentration, the concentration of those micelles that contain j solubilized molecules, and the average number of solubilized molecules per micelle, respectively. The last is simply given by

$$\bar{n} = \frac{[Py]_m}{[M]} = \frac{[Py]_m N_{agg}}{[surf]_{total} - c_{crit}} \tag{2}$$

where $[Py]_m$, N_{agg}, and $[surf]_{total}$ are the analytical concentration (i.e., the concentration based on the total solution volume) of pyrene that resides in the micellar pseudophase, the aggregation number of the micelles or the polymer-bound surfactant aggregates, and the total analytical surfactant concentration, respectively, and c_{crit} is the appropriate critical surfactant concentration, i.e., the cac in the case of polymer-bound aggregates, the cmc for polymer-free surfactant solutions, or c_{sat} + cmc − cac when one is concerned with the appearance of free micelles after the polymer-saturation point in polymer−surfactant mixtures.

According to Infelta and Grätzel,[39] the fluorescence intensities due to pyrene monomers and excimers solubilized in surfactant aggregates are, respectively,

$$I_m^{mon} = K_m \phi_m^{mon} R \sum_{j=1}^{\infty} \left(\frac{j}{R + j - 1} \right) \frac{[M_j]}{[M]} \tag{3a}$$

$$I_m^{e} = K_m \phi_m^{e} \sum_{j=2}^{\infty} \left(\frac{j(j-1)}{R + j - 1} \right) \frac{[M_j]}{[M]} \tag{3b}$$

where K_m is a proportionality factor involving the absorptivity as well as instrumental factors, ϕ_m^{mon} and ϕ_m^{e} are the monomer and excimer quantum yields inside the micelle, respectively, and R is a kinetic factor arising from the fluorescence mechanism. The subscript "m" emphasizes that these refer to pyrene in micelles (or bound aggregates as the case may be). If the surfactant concentration is low, a significant fraction of the fluorophores resides in the aqueous pseudophase and contributes mainly to the monomer emission intensity, as was discussed in our previous paper.[45] However, in this study we focus our analysis on sufficiently large surfactant concentrations such that both the excimer and the monomer fluorescence intensities arising from the aqueous pseudophase are negligible compared to those from the micellar pseudophase(s). Thus, the ratio of

monomer and excimer fluorescence intensities can be expressed here as

$$\frac{I^e}{I^{mon}} = \frac{\dfrac{\phi_m^e}{\phi_m^{mon}} \displaystyle\sum_{j=2}^{\infty} \left(\frac{j(j-1)}{R+j-1} \right) \frac{[M_j]}{[M]}}{R \displaystyle\sum_{j=1}^{\infty} \left(\frac{j}{R+j-1} \right) \frac{[M_j]}{[M]}} \tag{4}$$

Because of its relation to the Poisson distribution (eq 1) the I^e/I^{mon} ratio must depend on $\bar{n}$. By fixing the analytical pyrene concentration and gradually increasing the SDS concentration from below the cac to well beyond c_{sat} + cmc − cac, i.e., manipulating $\bar{n}$, we can determine the number of PEG-bound SDS aggregates and free SDS micelles in the solution, as well as the respective aggregation numbers, from the I^e/I^{mon} ratio.

The values of R and ϕ_m^{mon}/ϕ_m^e can be found by numerical analysis of the I^e/I^{mon} ratio versus micelle concentration relationship or by independent experiments. However, as we will discuss later, the model is quite insensitive to the values of these parameters. The model is dominated by the quantitative dependence of $\bar{n}$ on the surfactant concentration.

Experimental Section

Materials. PEG (molecular weight 10 000) was obtained from Polysciences, Inc. and was further purified by dissolving in methylene chloride (Fisher, ACS grade), then precipitating with ethyl ether (Fisher, ACS grade), and filtering with a glass filter. Finally, it was dried under vacuum at room temperature. We purchased SDS from Fluka Chemical Corp. (>99% pure), and further purified it by washing with hot acetone (Fisher, HPLC grade) more than three times, then drying under vacuum at room temperature. The surface tension measurements of purified SDS solutions showed no dip near the cmc (8.3 mM in deionized water). Pyrene was obtained from Aldrich Chemical Co. (optical grade, >99% pure) and used as received. All water was purified by reverse osmosis followed by treatment with a Milli-Q Plus system from Millipore Corp. We purchased methanol (ACS grade) from Fisher and used it as received.

Methods. For fluorescence measurements, aliquots of pyrene stock solutions in methanol were added to solutions that already contained SDS and PEG to prepare 5, 10, or 20 μM analytical pyrene concentrations. These SDS−PEG−pyrene solutions were allowed to equilibrate for at least 8 h after adding pyrene and then centrifuged at 3000 rpm for 1 h. Centrifuging removed the excess pyrene microcrystals from the low surfactant concentration samples.[45] Trace amounts of methanol in the pyrene solutions (maximum 0.2 vol %) do not affect the solubilization or fluorescence properties.[48,49,45] We measured the steady-state pyrene fluorescence emission with a Perkin-Elmer LS-5B fluorescence spectrometer, using 240 nm excitation and recording the emission spectrum between 270 and 750 nm. The excitation and emission slit widths were 5 and 3 nm, respectively. We used 10 mm path length quartz cuvettes and corrected for inner filter effects as described previously.[45]

For the UV−vis measurements of total solubilized pyrene, we added an excess of powdered pyrene to the SDS or SDS−PEG solutions. These were sonicated for more than 8 h and then centrifuged at 3000 rpm for 1 h to sediment excess pyrene. Supernatants were taken and diluted into standard 50 mM SDS solutions in order to assay the total solubilized pyrene concentration. Using a Hewlett-Packard 8451 diode array spectrophotometer, we measured the absorbance at 336 nm in quartz cuvettes and used the molar absorptivity of 2.06×10^{-5} M/cm to calculate the pyrene concentration. We measured this molar absorptivity for pyrene solubilized in micellar SDS solutions. Neither the PEG nor the SDS has significant absorbance at 336 nm.

Using a du Noüy ring tensiometer, we measured the surface tension of SDS and SDS−PEG solutions without pyrene to check the consistency of fluorescence and the classical surface tension method for detecting SDS−PEG binding. The temperature was 25 °C in all experiments.

Results and Discussion

Pyrene Solubilization in SDS Solutions. Before examining SDS−PEG mixtures, we first describe the solubilizing power and solubilization capacity of free SDS micelles in the absence of PEG. It is well-known that increasing the ionic strength decreases the cmc and increases N_{agg} in polymer-free SDS solutions. We exploit this behavior to examine the sensitivity of the I^e/I^{mon} ratio to changes in both N_{agg} and $\bar{n}$, as shown in Figure 2. In so doing, we test the applicability of the model assumptions, including the applicability of the Poisson distribution model to this system.

In the experiments summarized by Figure 2, the pyrene analytical concentration was fixed at 5 μM (approximately 7 times higher than its solubility limit in pure water) as we varied the total surfactant concentration in three sets of experiments conducted at either 0, 20 or 100 mM NaCl concentration. To analyze the excimer fluorescence data, we performed a least-squares regression analysis according to the model described by eqs 1, 2, and 4. We determined the appropriate critical concentration in eq 2, the cmc in this case, by UV absorbance, I_1/I_3 and I^e/I^{mon} data. Then, we treated R, ϕ_m^{mon}/ϕ_m^e, and N_{agg} as fitting parameters in the least-squares regression but we constrained the values of the two parameters derived from the fluorescence mechanism, R and ϕ_m^{mon}/ϕ_m^e, to be the same in all regressions. The best-fit values for R and ϕ_m^{mon}/ϕ_m^e were 0.8 and 1.9, respectively.

Table 1 summarizes micellization and solubilization parameters for PEG-free SDS solutions for the three different NaCl concentrations. For comparison, Table 1 also includes independent values for the cmc and aggregation number determined by static light scattering as reported by Phillips and Mysels.[50] Inspection of Table 1 confirms that micellization parameters obtained by excimer fluorescence spectroscopy are in excellent agreement with the light scattering results. This supports the applicability of the model, including the assumption of Poisson statistics.

In Figure 2a, each series of measurements follows a similar trend, namely a sharp increase in I^e/I^{mon} beginning at the cmc, passage through a maximum somewhat above the cmc, and a monotonic decrease as the surfactant concentration increases.

The effect of ionic strength on the cmc and also on solubilization capacities is immediately apparent in Figure 2a. The peak in I^e/I^{mon} results from the passage of $\bar{n}$ through a maximum. As we discussed in our previous paper,[45] this reflects micelle saturation and the nonlinear partitioning behavior at low surfactant/pyrene ratios. At SDS concentrations beyond this peak position, all available pyrene is completely solubilized, and further increases in SDS concentration simply decrease $\bar{n}$, i.e., the finite population of pyrene molecules is being diluted over an increasing number of micelles. Note also that, beyond the SDS concentration where the peak occurs, there are no solid pyrene microcrystals to be centrifuged. The increasing height

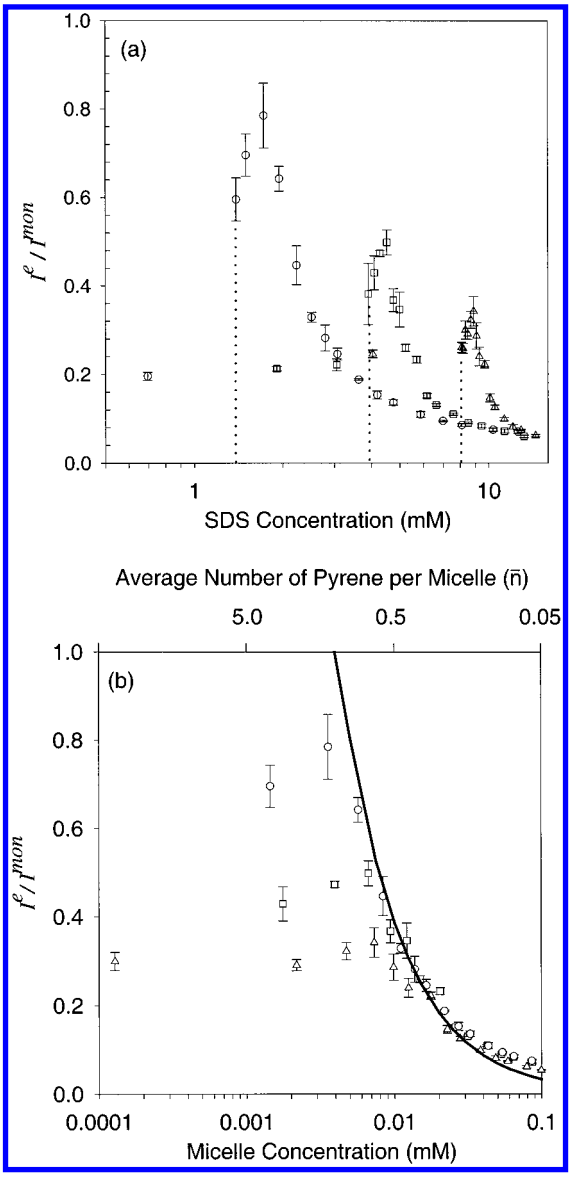

Figure 2. (a) Excimer to monomer fluorescence ratio dependence on the total SDS concentration at three different NaCl concentrations in the absence of PEG. Dotted lines indicate the cmc for each series of data. (b) The same data, plotted against the SDS micelle concentration. Symbols denote: triangles, 0 mM NaCl; squares, 20 mM NaCl; circles, 100 mM NaCl; line, Poisson distribution model.

TABLE 1: Solubilization Properties in SDS Solutions in the Absence of PEG

	free SDS micelles			
NaCl (mM)	cmc[a] (mM)	N_{agg}[a]	solubilizing power (Py/surfactant)	solubilization capacity[b] (Py/micelle)
0	8.33 ± 0.05 (8.1)	78 ± 1.1 (80)	$(6.8 \pm 0.1) \times 10^{-3}$	0.68 ± 0.18 (0.53 ± 0.01)
20	3.95 ± 0.03 (3.82)	86 ± 1.2 (94)	$(7.4 \pm 0.1) \times 10^{-3}$	0.74 ± 0.21 (0.64 ± 0.01)
100	1.35 ± 0.04 (1.39)	105 ± 5.6 (112)	$(7.9 \pm 0.1) \times 10^{-3}$	1.4 ± 0.52 (0.83 ± 0.05)

[a] Values for cmc and N_{agg} reported in parentheses are from Philips and Mysels.[50] [b] Solubilization capacities reported in parentheses are calculated as the product of solubilizing power and N_{agg}.

of the peak with increasing ionic strength reflects the increasing solubilization capacity.

To further test the suitability of our modeling approach, we examine the data in Figure 2a by replotting it against the micelle concentration [M], rather than the total surfactant concentration, as shown in Figure 2b. As eq 2 implies, the micelle concentration is dictated by the values of cmc and N_{agg}. Plotting the data in this way, equal values of [M] for any ionic strength correspond to equal values of $\bar{n}$ via eq 2, since 100% of the pyrene originally added is solubilized after the peak position. The data for all micelle concentrations greater than that corresponding to the maximum all collapse onto a single curve that is well matched by the Poisson distribution model.

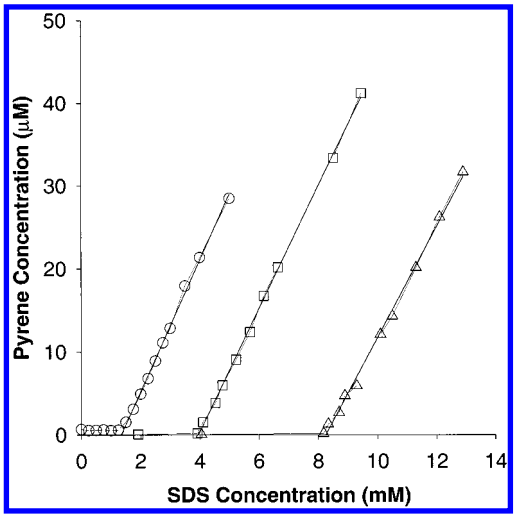

Figure 3. Solubilizing power of SDS micelles at different ionic strengths in the absence of PEG. Symbol assignments and corresponding slopes: triangles, 0 mM NaCl, 6.8 μM pyrene/mM SDS; squares, 20 mM NaCl, 7.4 μM pyrene/mM SDS; circles, 100 mM NaCl, 7.9 μM pyrene/mM SDS.

Note that the three data series in Figure 2b should not be expected to converge for micelle concentrations below their respective peak positions, because micelles that are present under those conditions are fully saturated with pyrene. Because of the dependence of the solubilization capacity on the NaCl concentration, lower NaCl concentrations must produce consistently lower values of I^e/I^{mon} for all micelle concentrations at which they are saturated with pyrene, i.e., before the peak.

Thus, we see that when we vary the ionic strength to systematically vary N_{agg}, I^e/I^{mon} depends only on $\bar{n}$, via the statistical distribution model. The only significant effect of N_{agg} is that it fixes [M] for a particular SDS concentration. This observation that excimer emission does not depend intrinsically on the aggregation number itself is important because it allows us to safely treat the parameters R and ϕ_m^e/ϕ_m^{mon} as constants in all of our experiments, even when micelle structures may be changing. In other words, the statistics of solubilizate distribution control the excimer fluorescence spectroscopy in SDS solutions. The altered composition of a micelle formed under different conditions has no chemical effect on pyrene fluorescence.

The increasing height of the peak with increasing ionic strength shows that the solubilization capacity increases with increasing aggregation number (see Table 1). From the value of $\bar{n}$ at the peaks, we determine solubilization capacities of 0.68 $\pm$ 0.18 pyrene per micelle at zero NaCl, 0.74 $\pm$ 0.21 pyrene per micelle at 20 mM NaCl, and 1.40 $\pm$ 0.52 pyrene per micelle at 100 mM NaCl. Note that we do not apply the model to data before the peak position, since the Poisson distribution cannot predict a peak.

Figure 3 shows the results of the UV−vis absorbance measurements of the total uptake of pyrene by SDS solutions of varying ionic strength. The solubilizing power is determined as the slope of the lines that begin at the cmc. This increases

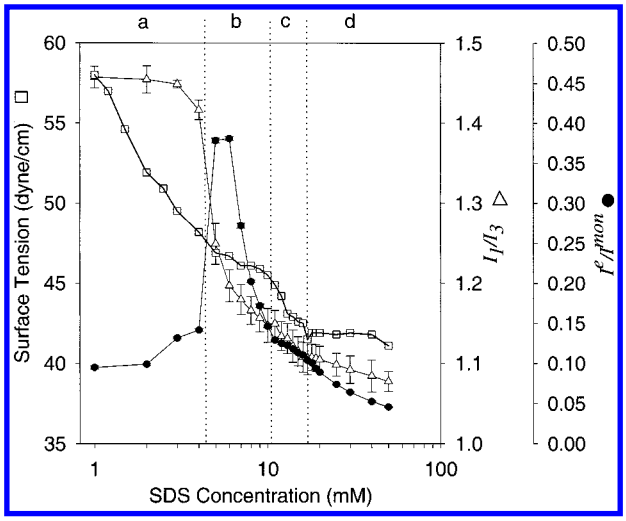

Figure 4. Surface tension and pyrene fluorescence behaviors in the presence of 0.1 wt % PEG. Pyrene concentration (for fluorescence measurements) was 20 μM. Symbols denote: squares, surface tension; circles, I^e/I^{mon}; triangles, I_1/I_3.

by 16%, from 6.8 to 7.9 mmol pyrene per mole SDS as the NaCl concentration increases from 0 to 100 mM. Since the micelles are loaded to their full solubilization capacities for all surfactant concentrations in these macroscopic solubilization experiments, we may also calculate the solubilization capacity from the UV−vis data simply by multiplying the solubilizing power by the aggregation number that we determined independently from the excimer fluorescence analysis. These values are reported together with those calculated directly from the excimer analysis in Table 1. Thus, we see that the solubilization capacity increases by 56%, from 0.53 pyrene per micelle to 0.83 pyrene per micelle as the NaCl concentration increases from 0 to 100 mM. Interestingly, on average not every micelle contains a pyrene molecule at saturation, but the fact that excimers do form indicates that a significant number of micelles contain two or more pyrene molecules at any given time.

The solubilization capacity values obtained from the absorbance and the fluorescence measurements agree fairly well at 0 and 20 mM NaCl, but not at 100 mM NaCl. The discrepancy may reflect the difficulty of precisely locating the peak position (i.e., the limiting value of $\bar{n}$) in Figure 2b at the highest ionic strength where the curve is steepest.

Pyrene Solubilization in SDS−PEG Mixtures. The general SDS−PEG binding behavior is mapped in Figure 4 and summarized in Table 2. Here, we compare the abilities of excimer fluorescence and I_1/I_3 ratio measurements to detect transitions in the SDS−PEG binding behavior with the ability of surface tension measurements to do the same. All the measurements shown in Figure 4 are without NaCl and contain 0.1 wt % PEG. Consistent with Goddard's results[3] for similar conditions, the surface tension data indicate that the cac is approximately 5 mM SDS and c_{sat} is approximately 12 mM SDS.

Compared to surface tension data, the cac is much more apparent in the I_1/I_3 and the I^e/I^{mon} measurements. Both indicate that the cac is approximately 4.4 mM, but both also suggest that the transition is not abrupt. The decrease in I_1/I_3 just below 4.4 mM indicates that there is some pyrene partitioning into an environment that is less polar than water. As should be expected, excimer fluorescence begins to become slightly more significant at the same SDS concentration where I_1/I_3 starts to decrease. We take the cac to be 4.4 ± 0.2 mM from UV absorbance measurement, and it is also where both fluorescence ratios change most sharply.

Other binding transitions are evident in both the surface tension and fluorescence data. Before quantitatively analyzing the fluorescence data, let us qualitatively discuss the effects of increasing SDS concentrations on the fluorescence behavior. We subdivide the SDS concentration range into four regimes (a−d) in Figure 4. In regime a both I_1/I_3 and I^e/I^{mon} are nearly constant, indicating that there are neither free micelles nor PEG-bound SDS aggregates, except toward the very end of this regime.

The boundary between regimes a and b is the cac. In regime b, we detect the onset of PEG−SDS complexation, producing micelle-like structures that can solubilize pyrene. The I^e/I^{mon} ratio increases until the SDS concentration reaches approximately 6 mM, at which point the number of the PEG-bound SDS aggregates becomes sufficiently large to solubilize all the pyrene in the system (20 μM in this experiment). Further increasing SDS beyond this point decreases $\bar{n}$ and therefore I^e/I^{mon}.

I_1/I_3 decreases monotonically throughout this entire regime, indicating that the pyrene microenvironment is becoming increasingly nonpolar on average. For SDS concentrations between the cac and 6 mM, this can be attributed to the increasing fraction of pyrene molecules that are transferring from the aqueous pseudophase into less polar PEG-bound SDS aggregates. That I_1/I_3 continues to decrease as the SDS concentration exceeds 6 mM SDS, even though the excimer data shows that all the pyrene is solubilized after 6 mM SDS, indicates that the microenvironmental polarity experienced by solubilized pyrene molecules within PEG-bound SDS aggregates depends on the average number of pyrene molecules contained within an aggregate.

The following mechanism is consistent with, though not necessarily proven by, the data after 6 mM SDS in regime b. Pyrene−pyrene interactions within a surfactant aggregate will affect the degree to which pyrene molecules must sample different microenvironments within the aggregate (e.g., aggregate core, palisade layer, headgroup region). When a finite population of pyrene molecules is diluted over an increasingly large population of aggregates, as occurs when the SDS concentrated is increased beyond 6 mM in Figure 4, pyrene−pyrene interactions must become less significant factors in determining the locus of solubilization. When only one pyrene molecule occupies an aggregate, selection of the thermodynamically optimal locus of solubilization within the aggregate is not influenced by pyrene−pyrene interactions. On the basis of I_1/I_3 ratios measured under such conditions (surfactant concentrations approaching c_{sat}), this locus evidently has a moderately low polarity. In contrast, under conditions where the aggregates are close to saturation, there is a larger probability that two or more pyrene molecules share an aggregate (as confirmed by the enhanced excimer emission near 6 mM SDS in Figure 4). Then pyrene−pyrene excluded volume repulsions will make it necessary for pyrene molecules to sample more regions of the aggregate, including those that are less thermodynamically attractive, such as the more polar, water-accessible regions near the headgroups. As a result, the average polarity and the average I_1/I_3 ratio is higher when the aggregates are saturated with pyrene than when the pyrene is diluted over a large number of aggregates.

Another possible explanation of the decreasing microenvironmental polarity in this concentration range is that the PEG-bound aggregates grow with increasing SDS concentration, but

TABLE 2: Solubilization Properties in SDS Solutions Containing 0.1 wt % PEG

NaCl (mM)	free SDS micelles solubilizing power (Py/surfactant)	PEG-bound SDS aggregates				
		cac (mM)	c_{sat} (mM)	N_{agg}	solubilizing power (Py/surfactant)	solubilization capacity[a] (Py/micelle)
0	$(7.6 \pm 0.1) \times 10^{-3}$	4.4 ± 0.2	12 ± 1	34 ± 1.2	$(12.8 \pm 0.5) \times 10^{-3}$	0.61 ± 0.16 (0.44 ± 0.02)
20	$(8.3 \pm 0.3) \times 10^{-3}$	2.0 ± 0.2	12 ± 1	44 ± 1.6	$(16.3 \pm 0.7) \times 10^{-3}$	0.68 ± 0.15 (0.72 ± 0.04)
100	$(8.7 \pm 0.3) \times 10^{-3}$	1.2 ± 0.12	11 ± 1	47 ± 1.7	$(17.0 \pm 0.4) \times 10^{-3}$	1.6 ± 0.65 (0.80 ± 0.03)

[a] Solubilization capacities reported in parentheses are calculated as the product of solubilizing power and N_{agg}.

this hypothesis is not consistent with the passage of I^e/I^{mon} through a maximum while I_1/I_3 decreases monotonically. The observed decrease in I^e/I^{mon} beyond 6 mM SDS argues that surfactant consumption in this range occurs by creation of new aggregates (so that $\bar{n}$ decreases) rather than growth of existing aggregates (in which case $\bar{n}$ and I^e/I^{mon} would not change). As will be discussed below, the excimer data in this regime is well described by a constant aggregation number.

Upon entering regime c, the SDS concentration now exceeds c_{sat}, the concentration at which the PEG is saturated by SDS binding. In regime c the I^e/I^{mon} ratio continues to decrease, albeit less rapidly than in regime b. This indicates that the rate (with respect to SDS concentration) at which new SDS aggregates appear has decreased compared to regime b. Here, most of the newly added SDS molecules probably go into the aqueous pseudophase as free monomers. This would be consistent with a drop in surface tension across regime c. Yet, the decrease in I^e/I^{mon} reveals that despite the expectation that no new aggregates of any kind should be formed between c_{sat} and c_{sat}+ cmc − cac, it appears that new aggregates are indeed formed. According to expectation, if no new aggregates were to form, then $\bar{n}$ and I^e/I^{mon} would have remained constant throughout regime c. The I_1/I_3 ratio also decreases throughout regime c, indicating either that the newly forming aggregates provide a more nonpolar microenvironment than the preexisting ones formed in regime b or else the pyrene molecules slip into increasingly nonpolar regions of all aggregates as the finite pyrene population continues to be distributed over an increasing number of aggregates.

Entering regime d where the SDS concentration exceeds c_{sat} + cmc − cac, the I^e/I^{mon} ratio decreases rapidly again because free SDS micelles are being formed, thereby decreasing $\bar{n}$ values. I_1/I_3 continues to decrease. As the partitioning between PEG-bound SDS aggregates versus free SDS micelles sways in favor of free micelles, the microenvironmental polarity continuously approaches the lower value that is characteristic of free SDS micelles. (In the absence of PEG, we observed that I_1/I_3 is 1.01 for pyrene completely solubilized in free SDS micelles, whereas the lower limit of I_1/I_3 is approximately 1.15 in PEG-bound SDS aggregates.)

Previously, van Stam et al.[51] concluded from fluorescence quenching data on similar systems that added surfactant is consumed by the growth of all aggregates simultaneously and not by the nucleation of new aggregates. This is not consistent with our excimer fluorescence data. In the aggregate growth mechanism, $\bar{n}$ and thus I^e/I^{mon} would stay constant during the binding regime b since I^e/I^{mon} only depends on $\bar{n}$ and not on N_{agg} per se; however, our I^e/I^{mon} data indicate that $\bar{n}$ is indeed decreasing and thus the number of aggregates is increasing as more SDS molecules are bound in this regime. A combined nucleation and growth mechanism might be more significant in regime c. There we initially expected neither nucleation nor growth of aggregates. Instead, we found that $\bar{n}$ did indeed

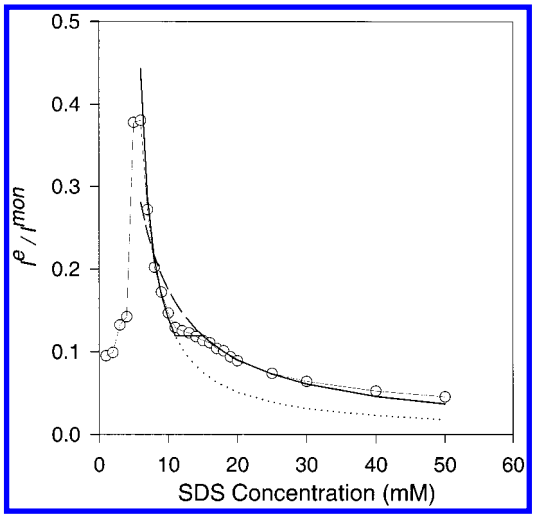

Figure 5. Comparison of model and data for I^e/I^{mon} fluorescence ratio in the presence of 0.1 wt % PEG. Solid curve, model with $N_{agg,bound} = 34$ and $N_{agg,free} = 83$; dashed curve, model where all aggregates have $N_{agg} = N_{agg,free} = 83$; dotted curve, model where all aggregates have $N_{agg} = N_{agg,bound} = 34$.

decrease with increasing SDS concentration, but not as rapidly as in the "binding" regime b. The fluorescence behavior would also be consistent with the formation of both free micelles and bound aggregates in regime c.

Now we discuss the quantitative analysis, focusing on the 0 mM NaCl data. Results for all three NaCl concentrations examined are summarized in Table 2. From the I^e/I^{mon} ratio, we determine the aggregation numbers for both the PEG-bound SDS aggregates and the free SDS micelles that coexist with them at high SDS concentrations. In our analysis we assume first that the aggregation number of the PEG-bound SDS aggregates is constant throughout regime b; second, all additional SDS added in regime c goes into solution as monomeric surfactant (a simplifying model assumption made despite the previous discussion), while all of the PEG-bound aggregates generated in regime b still exist unchanged; and third, that only free micelles are generated in regime d, while all PEG-bound aggregates generated in regime b still exist unchanged.

Since the aggregation numbers and the appropriate critical concentrations together fix the total aggregate concentration [M] for any given SDS concentration, we can determine aggregation numbers by regressing the I^e/I^{mon} data (example shown in Figure 5) against the excimer fluorescence and material balance model (eqs 1, 2, and 4). As discussed above in the context of the PEG-free SDS solutions, the values of R and ϕ_m^e/ϕ_m^{mon} were constrained to be the same in all regressions ($R = 0.8$ and $\phi_m^e/\phi_m^{mon} = 1.9$). Again we emphasize that the regressed values of R and ϕ_m^e/ϕ_m^{mon} were highly coupled, since I^e/I^{mon} is not very sensitive to the values of these constants, and is instead dominated by the partitioning statistics via the dependence of $\bar{n}$ on the SDS

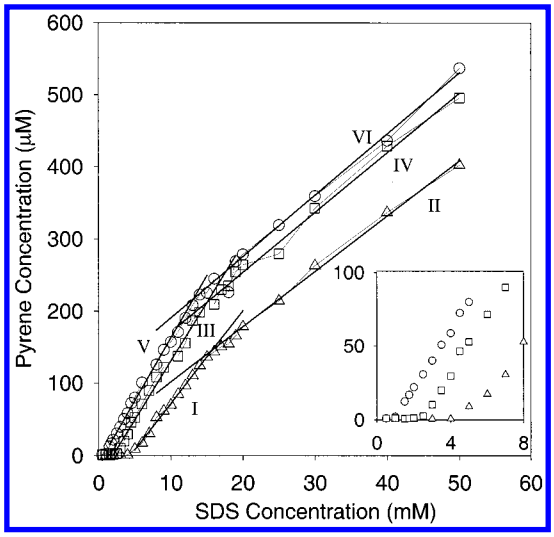

Figure 6. Effect of NaCl on pyrene solubilizing power in SDS solutions containing 0.1 wt % PEG. Symbols denote: triangles, 0 mM NaCl; squares, 20 mM NaCl; circles, 100 mM NaCl. Slopes: I, 12.8 mM pyrene/M SDS; II, 7.6 mM Py/M SDS; III, 16.3 mM Py/M SDS; IV, 8.3 mM Py/M SDS; V, 17.0 mM Py/M SDS; VI, 8.7 mM Py/M SDS. The inset shows the low concentration data to better observe the cac values.

concentration. Recall that this was well demonstrated experimentally in Figure 2 for free SDS micelles in the absence of PEG.

By regressing the data in regime b where only PEG-bound SDS aggregates exist, we found $N_{agg,bound} = 34 \pm 1$ for the PEG-bound aggregates in the absence of NaCl. The appropriate critical concentration used to calculate $\bar{n}$ from eq 2 was $c_{crit} =$ cac $= 4.4$ mM. The assertion that only PEG-bound aggregates solubilize pyrene in this regime, that falls between cac and c_{sat}, will also be apparent when examining solubilization power data, presented below in Figure 6. Knowing the value of N_{agg}, we calculate the value of $\bar{n}$ at the maximum in the plot of I^e/I^{mon} versus SDS concentration. This is the solubilization capacity. Thus, we find that the solubilization capacity of PEG-bound SDS aggregates is 0.61 ± 0.04 in the absence of NaCl.

In regime c, the PEG-bound SDS aggregate concentration was held constant at the value corresponding to the end of regime b. Thus, I^e/I^{mon} remained constant in the model analysis throughout regime c. In regime d, the total micelle concentration [M] for any given SDS concentration was the sum of the concentrations of PEG-bound aggregates $[M]_{bound}$ plus free micelles $[M]_{free}$. The concentration of PEG-bound aggregates was still held constant at the value corresponding to the end of regime b. Only the free micelle concentration was allowed to increase with increasing SDS concentration. In this case, the appropriate critical concentration used to calculate the *free* micelle concentration in eq 2 was $c_{crit} = c_{sat} +$ cmc $-$ cac $=$ 15.9 mM. Thus, in regime d, eq 2 is replaced by

$$\bar{n} = \frac{[Py]}{[M]_{bound} + [M]_{free}} = \frac{[Py]}{\frac{c_{sat} - cac}{N_{agg,bound}} + \frac{[SDS] - (c_{sat} + cmc - cac)}{N_{agg,free}}} \quad (5)$$

where [Py] is the total analytical pyrene concentration, since it is 100% solubilized throughout regime d, and $N_{agg,bound}$ and $N_{agg,free}$ refer to the aggregation numbers of PEG-bound aggregates and free SDS micelles, respectively. $N_{agg,bound}$ was simply the value calculated from the analysis of regime b above.

Applying eqs 1,4, and 5 to the excimer data in regime d, we found the aggregation number of the free SDS micelles was $N_{agg,free} = 83 \pm 6$ in the absence of NaCl. This is consistent with the value of $N_{agg} = 78$ measured for SDS in the absence of PEG.

Both $N_{agg,bound}$ and $N_{agg,free}$ agree quite well with other published results. Reported aggregation numbers for free SDS micelles in deionized water range from 69 to 80 as measured by static or dynamic fluorescence quenching or by light scattering.[48,50,51] Aggregation numbers for PEG-bound SDS aggregates range from 35 to 52.[10,11,13,49]

It should also be noted that the shape of the I^e/I^{mon} ratio curve cannot be explained by using a single aggregation number to describe both the PEG-bound aggregates and the free micelles. As is also shown in Figure 5, an aggregation number that adequately describes the high SDS concentration data, where free micelles dominate, cannot describe the data at low concentrations, where PEG-bound aggregates dominate, and vice-versa.

Figure 6 shows the results of solubilizing power measurements for SDS−PEG mixtures at different NaCl concentrations. The onset of solubilization occurs at the cac. In all cases, the values of the cac indicated by these ultraviolet absorbance measurements are consistent with those determined by fluorescence spectroscopy. The transition from solubilization by PEG-bound aggregates to solubilization by free micelles is immediately apparent from the change in slope that occurs at $c_{sat} +$ cmc $-$ cac. The macroscopic solubilizing power measurements do not give any obvious indication of the aggregation processes that fluorescence spectroscopy revealed in regime c just beyond c_{sat}.

Tables 1 and 2 summarize the aggregation and solubilization properties of free SDS micelles and of PEG-bound SDS aggregates at three different NaCl concentrations. For each NaCl concentration we examined, the solubilizing power of the PEG-bound aggregates is significantly higher than that of the free micelles. Aggregation numbers of PEG-bound aggregates are approximately half as large as those of free SDS micelles.

The solubilizing powers of the free micelles that form above $c_{sat} +$ cmc $-$ cac in the presence of PEG are slightly higher than the values measured for SDS micelles in polymer-free solutions (Figures 3 and 6). The differences are small but exceed the experimental uncertainty limits.

Similar to SDS micelles formed in the absence of PEG, the solubilizing power of free micelles that form at high SDS concentrations in the presence of PEG is only weakly affected by NaCl concentration, changing by 14%, from 7.6 to 8.7 mmol pyrene per mole SDS as the NaCl concentration changes from 0 to 100 mM. In contrast, the solubilizing power of PEG-bound aggregates increases by 33% for the same change in ionic strength, from 12.8 to 17.0 mmol pyrene per mole SDS.

As was the case with PEG-free SDS micelles, the solubilization capacities of PEG-bound SDS aggregates that were calculated directly from excimer fluorescence data agree reasonably well with those calculated as the product of the solubilizing power and the aggregation number at 0 and 20 mM NaCl, but not at 100 mM NaCl. Regardless of the way in which it was calculated, the solubilization capacity of PEG-bound SDS aggregates was not significantly different from that of free SDS micelles for any NaCl concentration examined. This is why PEG-bound SDS provides a greater solubilizing power than free SDS.

While a bound aggregate can carry as much pyrene as a free micelle, the smaller aggregation number of the bound aggregate provides for a greater concentration of distinct surfactant aggregates for a given surfactant concentration. The net effect of the PEG chains is actually to promote pyrene solubilization, even though we and others[51] find no evidence for a direct interaction between pyrene and PEG itself. For example, there is no micropolarity (I_1/I_3 ratio) or excimer effect in SDS-free PEG solutions.

Hypotheses for the Molecular Basis of PEG Effects on Pyrene Solubilization. The interesting feature of PEG-bound aggregates is that they have much smaller aggregation numbers than free micelles, yet their solubilization capacities are almost the same. From the study of Cabane[7] it is known that the PEG chain interacts with methylene units that are very close to the SDS headgroups in these complexes, playing a role similar to a cosurfactant. SANS measurements indicate that the PEG-bound SDS aggregates are similar in size, 20 Å radius spheres, to the micelles formed by pure SDS solutions at low ionic strengths.[8] Thus, if PEG-bound aggregates have fewer surfactants but occupy the same volume, the PEG chain may be expanding the pyrene-accessible volume in the palisade layer. The greatest linear dimension of pyrene is approximately 10 Å and therefore may be accommodated in the palisade layer of such micelles. Expansion of the accessible volume in the palisade layer relative to that of free SDS micelles is supported by the observation, based on limiting values of I_1/I_3 ratios, that the least polar microenvironment sensed by pyrene in SDS−PEG aggregates is still more polar than what is sensed by pyrene solubilized in free SDS micelles. This might indicate that PEG-bound aggregates have greater available volume for water. Since the thermodynamic driving force for pyrene to partition into a surfactant aggregate must still be strong despite the presence of some water and PEG segments beneath the headgroups, the greater accessible volume may allow these aggregates to accommodate more pyrene than would otherwise be expected based on their aggregation numbers alone.

The other major effect of PEG is to increase the sensitivity of the solubilizing power to changes in ionic strength. For the solubilization of Sudan Red B dye in dodecylpyridinium chloride micellar solutions at different ionic strengths (no polymer present), Ikeda and Maruyama[28] found that the solubilizing power was independent of ionic strength, while the solubilization capacity changed in proportion to the aggregation number of spherical micelles when the ionic strength was changed. Pyrene solubilization by free SDS micelles conforms to this pattern. Since pyrene solubilization is believed to occur in the palisade layer just beneath the surface of the SDS micelle,[52,53] this is to be expected. The micelle surface area, and thus the volume of the palisade layer and solubilization capacity, is proportional to the aggregation number.

In contrast, pyrene solubilization in PEG-bound SDS aggregates does not follow the Ikeda and Maruyama pattern. Both the solubilizing power and solubilization capacity increase significantly with increasing ionic strength. Our data show that the maximum extent of SDS binding to PEG also depends on the ionic strength. The maximum average number of micelles bound per 10 000 Da PEG chain increases from 2.1 to 2.6 when the NaCl concentration increases from 0 to 100 mM. In terms of the total amount of bound SDS, the PEG-saturation limit increases from 2.1 to 3.1 g of SDS per gram of PEG when the NaCl concentration increases from 0 to 100 mM. These values are comparable to the results of Cabane and Duplessix[8,9] and Gao et al.[54] The increase in the amount of SDS bound at saturation reflects the decrease in electrostatic repulsions between neighboring SDS aggregates on a single chain. Both the number of bound aggregates per chain and their solubilization capacities increase as the ionic strength increases. Both of these factors favor solubilization. There may also be more subtle effects induced by increasing the ionic strength that are not readily addressable by our methods. As electrostatic repulsions between the sulfate headgroups are weakened by increasing ionic strength, perhaps the intermingling of surfactants and polymer segments in the bound aggregates changes in a way that favors solubilization.

Conclusions

Pyrene excimer fluorescence is a useful method for quantifying solubilizate micropartitioning among coexisting surfactant pseudophases in polymer−surfactant mixtures. A single set of measurements identifies polymer−surfactant binding transitions and also provides the solubilization capacities and aggregation numbers of PEG-bound SDS aggregates and free SDS micelles. Overall, we found that PEG-bound SDS aggregates are more effective than free micelles at solubilizing pyrene.

PEG increases the solubilizing power of SDS for pyrene by decreasing the aggregation number of bound aggregates, thereby producing a greater number of aggregates, while not significantly altering their solubilization capacity for pyrene. A simpler but equally important effect of PEG binding is that solubilization commences at significantly lower total SDS concentrations in the presence of PEG, since the cac is less than the cmc.

Compared to free SDS micelles, the solubilizing power of PEG-bound SDS aggregates is significantly more sensitive to ionic strength. Increasing ionic strength significantly increases both the solubilizing power and solubilization capacity of PEG-bound SDS aggregates. This may provide a mechanism to tune solubilization behaviors in complex fluid formulations. At the very least, it is useful to know that adding small amounts of PEG makes it possible to solubilize comparable amounts of pyrene with significantly less surfactant. For the case of 0.1 wt % PEG, the concentration of SDS needed to increase the solubility of pyrene by 1 order of magnitude is cut approximately by a factor two.

It remains to be determined to what extent the overall enhancement of pyrene solubilization by SDS−PEG binding may be generalized to other hydrocarbons. We would anticipate that the tendency of PEG to decrease the aggregation number of bound aggregates is likely to be independent of the type of solubilizate and should therefore always contribute to a net increase in the macroscopic solubilization power for other hydrocarbons. In that case, whether such an enhanced solubilizing power is realized would depend on how PEG-binding affects the microscopic solubilization capacities for those hydrocarbons. This would depend on the preferred locus of solubilization for that hydrocarbon relative to the near-headgroup region where PEG segments preferentially reside and would also depend of course on the possibility of strong hydrocarbon−PEG interaction energies.

Acknowledgment. This material is based on work supported by the National Science Foundation under Grant CTS-9623849.

References and Notes

(1) Goddard, E. D., Ananthapadmanabhan, K. P., Eds. *Interactions of Surfactants with Polymers and Proteins*; CRC Press: Boca Raton, FL, 1993.

(2) Robb, I. D. Polymer/surfactant interactions. In *Anionic surfactants: physical chemistry of surfactant action*; Lucassen-Reynders, E. H., Ed.; M. Dekker: New York, 1981; p 109.

(3) Goddard, E. D. *Colloids Surf.* **1986**, *19*, 255.
(4) Saito, S. Polymer-surfactant interactions. In *Nonionic surfactants: physical chemistry*; Schick, M. J., Ed.; M. Dekker: New York, 1987; p 881.
(5) Winnik, F. M.; Regismond, S. T. A. *Colloids Surf., A* **1996**, *118*, 1.
(6) Jones, M. N. *J. Colloid Interface Sci.* **1967**, *23*, 36.
(7) Cabane, B. *J. Phys. Chem.* **1977**, *81*, 1639.
(8) Cabane, B.; Duplessix, R. *J. Phys.* **1982**, *43*, 1529.
(9) Cabane, B.; Duplessix, R. *Colloids Surf.* **1985**, *13*, 19.
(10) Francois, J.; Dayantis, J.; Sabbadin, J. *Eur. Polym. J.* **1985**, *21*, 165.
(11) Lissi, E. A.; Abuin, E. *J. Colloid Interface Sci.* **1985**, *105*, 1.
(12) Cabane, B.; Duplessix, R. *J. Phys.* **1987**, *48*, 651.
(13) Witte, F. M.; Engberts, J. B. F. N. *Colloids Surf.* **1989**, *36*, 417.
(14) Hu, Y. Z.; Zhao, C. L.; Winnik, M. A.; Sundararajan, P. R. *Langmuir* **1990**, *6*, 880.
(15) Quina, F.; Abuin, E.; Lissi, E. *Macromolecules* **1990**, *23*, 5173.
(16) Brown, W.; Fundin, J.; Miguel, M. d. G. *Macromolecules* **1992**, *25*, 7192.
(17) Dubin, P. L.; Gruber, J. H.; Xia, J.; Zhang, H. *J. Colloid Interface Sci.* **1992**, *148*, 35.
(18) Maltesh, C.; Somasundaran, P. *Langmuir* **1992**, *8*, 1926.
(19) Lin, M. Y.; Sinha, S. K.; Chari, K. *J. Phys. IV* **1993**, *3*, 153.
(20) Maltesh, C.; Somasundaran, P. *J. Colloid Interface Sci.* **1993**, *157*, 14.
(21) Yekta, A.; Duhamel, J.; Brochard, P.; Adiwidjaja, H. *Macromolecules* **1993**, *26*, 1829.
(22) Chari, K.; Antalek, B.; Lin, M. Y.; Sinha, S. K. *J. Chem. Phys.* **1994**, *100*, 5294.
(23) Ruzza, A. A.; Froehner, S. J.; Minatti, E.; Nome, F.; Zanette, D. *J. Phys. Chem.* **1994**, *98*, 12361.
(24) Minatti, E.; Zanette, D. *Colloids Surf., A* **1996**, *113*, 237.
(25) Zanette, D.; Ruzza, A. A.; Froehner, S. J.; Minatti, E. *Colloids Surf., A* **1996**, *108*, 91.
(26) Gjerde, M. I.; Nerdal, W.; Hoiland, H. *J. Colloid Interface Sci.* **1998**, *197*, 191.
(27) Wang, Y.; Han, B.; Yan, H.; Cooke, D. J.; Lu, J. *Langmuir* **1998**, *14*, 6054.
(28) Ikeda, S.; Maruyama, Y. *J. Colloid Interface Sci.* **1994**, *166*, 1.
(29) Saito, S. *Kolloid, Z. Z. Polym.* **1967**, *215*, 16.
(30) Arai, H.; Horin, S. *J. Colloid Interface Sci.* **1969**, *30*, 372.
(31) Horin, S.; Arai, H. *J. Colloid Interface Sci.* **1970**, *32*, 547.
(32) Arai, H.; Murata, M.; Shinoda, K. *J. Colloid Interface Sci.* **1971**, *37*, 223.
(33) Tokiwa, F.; Tsujii, K. *Bull. Chem. Soc. Jpn.* **1973**, *46*, 2684.
(34) Abuin, E. B.; Scaiano, J. C. *J. Am. Chem. Soc.* **1984**, *106*, 6274.
(35) Binana-Limbele, W.; Zana, R. *Macromolecules* **1987**, *20*, 1331.
(36) Chu, D. Y.; Thomas, J. K. *Adv. Chem. Ser.* **1989**, *223*, 325.
(37) Sudbeck, E. A.; Dubin, P. L.; Curran, M. E.; Skelton, J. *J. Colloid Interface Sci.* **1991**, *142*, 512.
(38) Kalyanasundaram, K.; Thomas, J. K. *J. Am. Chem. Soc.* **1977**, *99*, 2039.
(39) Infelta, P. P.; Graetzel, M. *J. Chem. Phys.* **1979**, *70*, 179.
(40) Infelta, P. P. *Chem. Phys. Lett.* **1979**, *61*, 88.
(41) Almgren, M.; Leofroth, J. E.; van Stam, J. *J. Phys. Chem.* **1986**, *90*, 4431.
(42) Gehlen, M. H.; Van der Auweraer, M.; Reekmans, S.; Neumann, M. G.; De Schryver, F. C. *J. Phys. Chem.* **1991**, *95*, 5684.
(43) Bales, B. L.; Stenland, C. *J. Phys. Chem.* **1993**, *97*, 3418.
(44) Barzykin, A. V.; Tachiya, M. *J. Phys. Chem.* **1994**, *98*, 2677.
(45) Kim, J.-H.; Domach, M. M.; Tilton, R. D. *Colloids Surf., A* **1999**, *150*, 53.
(46) Hunter, T. F. *Chem. Phys. Lett.* **1980**, *75*, 152.
(47) Kim, J.-H. Pyrene Solubilization in Micelles and Polymer−Surfactant Complexes. Ph. D. Thesis, Carnegie Mellon University, 1999.
(48) Grieser, F.; Tausch-Treml, R. *J. Am. Chem. Soc.* **1980**, *102*, 7258.
(49) Edwards, D. A.; Luthy, R. G.; Liu, Z. *Environ. Sci. Technol.* **1991**, *25*, 127.
(50) Phillips, J. N.; Mysels, K. J. *J. Phys. Chem.* **1955**, *59*, 325.
(51) van Stam, J.; Almgren, M.; Lindblad, C. *Prog. Colloid Polym. Sci.* **1991**, *84*, 13.
(52) Graetzel, M.; Kalyanasundaram, K.; Thomas, J. K. *J. Am. Chem. Soc.* **1974**, *96*, 7869.
(53) Rodgers, M. A. J.; Da Silva e Wheeler, M. E. *Chem. Phys. Lett.* **1976**, *43*, 587.
(54) Gao, Z.; Wasylishen, R. E.; Kwak, J. C. T. *J. Phys. Chem.* **1991**, *95*, 462.